ChemComm

Accepted Manuscript

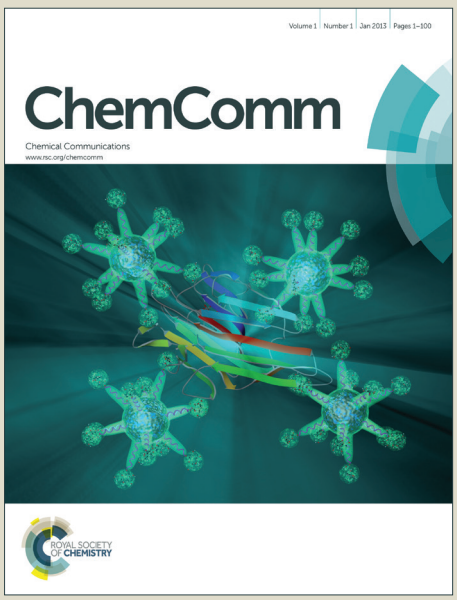

ROYAL SOCIETY OF CHEMISTRY

www.rsc.org/chemcomm

ChemComm

RSCPublishing

COMMUNICATION

Facile One-pot Synthesis of Porphyrin Based Porous Polymer Networks (PPNs) as Biomimetic Catalysts

Cite this: DOI: 10.1039/xoxxoooooox

Lanfang Zou,[a] Dawei Feng,[a] Tian-Fu Liu,[a] Ying-Pin Chen,[a,b] Stephen Fordham,[a] Shuai Yuan,[a] Jian Tian[a] and Hong-Cai Zhou*[a,b]

Received ooth January 2012,
Accepted ooth January 2012

DOI: 10.1039/xoxxoooooox

www.rsc.org/

Stable porphyrin based porous polymer networks, PPN-23 and PPN-24, have been synthesized through a facile one-pot approach by the aromatic substitution reactions of pyrrole and aldehydes. PPN-24(Fe) performs high catalytic efficiency as a biomimetic catalyst for the oxidation reaction of 2, 2'-azino-bis(3-ethylbenzthiazoline-6-sulfonic acid) (ABTS) in the presence of H_2O_2.

Catalytic activity of metalloprophyrin complexes have been extensively studied since the discovery of the heme-containing enzymes, cytochrome P450[1]. Inspired by the porphyrin core as the active site in cytochrome P450, many metalloporphyrin catalysts for hydroxylation, cyclopropanation, olefination, C-H insertion and N-H insertions have been explored.[2] Using synthetic systems to mimic natural enzymes with high catalytic activity has been a sought-after goal in the past decade. Direct application of the metalloporphyrin complexes in aqueous solution is usually challenging due to the formation of catalytically inactive dimers in the oxidizing reaction media.[3] With this consideration, various methods have been developed to heterogenize metalloporphyrin catalyst, including covalent bond formation, ion-pair formation, encapsulation or immobilization on supports such as zeolites, clays or mesoporous silica.[4] However, these methods usually dilute the density of active sites,[5] yield unwelcome interactions between substrate and catalyst, and lead to leaching of the complexes from substrate.[6]

As an alternative solution, advanced porous materials have been demonstrated as promising candidates to heterogenize metalloporphyrin because of their tuneable properties, high surface areas and controllable porosity. In the last two decades, metal-organic frameworks (MOFs), a novel category of porous materials, have been extensively investigated in scientific and technological research due to their potential application in many fields, such as gas storage[7], gas separation[8], sensors[9] and catalysis[10]. Recently, porphyrin derivatives have been introduced into MOFs by either linker modification or encapsulation.[10b, 11] MOFs possess many advantages, such as large surface area, tuneable structures, and feasible platform for post-synthetic modifications. However, most MOFs, constructed with soft Lewis acids (metal ions) and hard Lewis bases (carboxylates), suffer from limited stability, which highly restrained their potential in industry applications. Porous polymer networks (PPNs), hyper-cross linked organic polymers based on covalent-bonds, have provided an alternative way to construct functional porous materials with extremely high chemical and thermal stability.[12] Some research has been focused on synthesizing PPN materials with metalloporphyrin active centers utilizing pre-synthesized metalloporphyrin monomers *via* either C-C cross coupling reactions using Pd-catalyst or condensation with tetra(4-aminophenyl)methane.[13] Nevertheless, their synthetic methodologies are usually not scalable due to the complicated synthesis procedure for the monomers and the requirement of expensive metal catalysts for polymerization. Preparation of porphyrinic porous organic polymers (POPs) with 2D planar structure via bottom-up strategy has been initially reported by Bhaumik *et al*.[14] However, incorporation of porphyrinic active site into 3D porous framework through the one-pot facile synthesis was absence thus far.

Herein, we report a facile one-pot synthetic method to produce large scale metalloporphyrin containing porous polymer networks, named **PPN-23** and **PPN-24** (Fig. 1), of which **PPN-24** is the firstly reported 3D porphyrin based PPNs obtained by using this bottom-up synthetic strategy. This unique methodology is based on the extended condensation reaction between pyrrole and aromatic aldehydes including benzene-1, 3, 5-tricaialdehyde[15] (**PPN-23**) and tetrakis(4-formylphenyl)silane[16] (**PPN-24**). This condensation process yields black fluffy PPNs with high porosity, excellent thermal and chemical stability without the requirement of inert atmosphere or expensive catalysts. Moreover, the synthetic procedure is very cost- and time-efficient and the final material can be easily functionalized with various metal ions, such as iron(III), zinc(II), copper(II) and cobalt(II), through an effortless post-synthetic modification reaction.[10b] The catalytic activity of **PPN-24(Fe)** has been demonstrated by catalytic oxidation of 2, 2'-azino-bis(3-ethylbenzthiazoline-6-sulfonic acid) (ABTS) in the presence of H_2O_2. The catalytic activity of **PPN-24(Fe)** demonstrates the feasibility of precisely designing stable porous polymer materials to be applied for mimicking heme-based protein applications.

The synthesis was accomplished by treatment of pyrrole with benzene-1, 3, 5-tricaialdehyde (**PPN-23**) or tetrakis(4-formylphenyl)silane (**PPN-24**) in refluxed propionic acid media for

12 hours. Under acidic condition, aromatic aldehydes were first activated through protonation, followed by electrophilic aromatic substitution of the activated carbon atoms of pyrrole, and further condensation to yield macrocyclic porphyrin building blocks with-

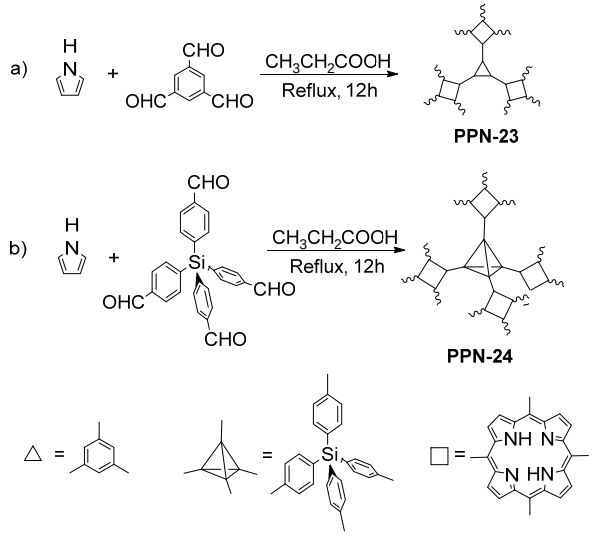

Fig. 1 Synthetic strategy of a) **PPN-23** and b) **PPN-24**: (Simplified using provided symbols).

-free aldehyde groups.[17] This condensation process repeats until the finish of the polymerization. After the reaction, black fluffy powder was collected, washed and dried to afford the **PPN-23** and **PPN-24**. FT-IR was employed to confirm the formation of porphyrin networks (in Fig. S6 and Fig. S7). Bands corresponding to 1720-1740 cm^{-1} (C=O stretching) are absent, suggesting all the aldehyde starting materials have been consumed in the polymerization reaction. The strong bands observed at 3317 cm^{-1}, 969 cm^{-1} and 802 cm^{-1} can be attributed to the characteristic stretching, bending and rocking vibrations of N-H bonds in porphyrin center, confirms the formation of microporous porphyrin networks. Field-emission scanning electron microscopy (FE-SEM) images show that **PPN-23** and **PPN-24** are composed of agglomerated sphere-shaped particles with sizes ranging from 1.0 to 3.2 μm in diameter (Fig. 2).

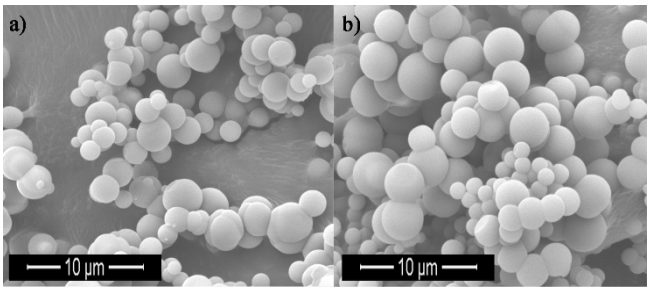

Fig. 2 SEM images of a) **PPN-23** and b) **PPN-24**.

Porosities of these PPNs have been established from the N_2 sorption analysis at 77 K. As evident from Fig. 3, both **PPN-23** and **PPN-24** exhibit type I isotherm, typical for microporous solids, where a steep gas uptake at low relative pressure and a mostly flat extrapolation in the intermediate sections of P/P^o are observed. N_2 uptakes of 102 $cm^3\ g^{-1}$ and 187 $cm^3\ g^{-1}$ have been obtained for **PPN-23** and **PPN-24**, respectively. The Brunauer-Emmett-Teller (BET) surface areas for **PPN-23** and **PPN-24** are 271 $m^2\ g^{-1}$ and 478 $m^2\ g^{-1}$, respectively (Langmuir surface areas 426 $m^2\ g^{-1}$ and 754 $m^2\ g^{-1}$, respectively), suggesting the permanent porosity of **PPN-23** and **PPN-24**. Density Functional Theory (DFT) pore size distribution analysis based on the N_2 isotherm at 77 K indicates the pore size of **PPN-23** is uniformly distributed around 13 Å, while **PPN-24** is around 10 Å and 11.8 Å (Fig. S4, 5). Even though these materials do not possess a long-range spatial periodicity, the narrowly distributed pore size indicates that they have ordered arrangements in a short range with permanent porosity after activation.[18]

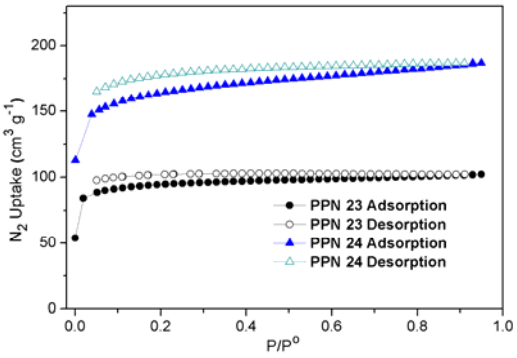

Fig. 3 N_2 isotherms for **PPN-23** and **PPN-24** at 77 K, 1 atm.

PPN-24 was taken as an example for stability test. The high thermal stability of **PPN-24** was confirmed by thermogravimetric analyzer (TGA) measurement (Fig. S8). During the departure of the guest molecules below 70 °C, about 10% weight loss was observed. From the phase transition a decomposition temperature of around 320 °C is observed for the fresh sample. Moreover, the chemical stability was tested through treatment with water (Fig. S9). After treatment with water for 36 hours, samples were measured by N_2 sorption at 77K after typical activation procedures. A reduction of the N_2 sorption capacity of less than 15% was observed, suggesting only a slight destroy of framework during these treatments. The excellent chemical stability can be ascribe to the strong covalent-bond connections, which endow the framework with high stability in aqueous solution. Both the thermal and chemical stability of **PPN-24** boost their further applications, especially in biomimetic catalysis.

To demonstrate these porphyrin based PPNs are ideal platform for heterogeneous biomimetic catalysis, we post-synthetically modified **PPN-24** through the insertion of Fe(III) in porphyrin center. The as-synthesized **PPN-24** was mixed with $FeCl_2$ (high reaction rate than $FeCl_3$) in DMF and heated at 100 °C for 12 hours to afford the catalytically active species **PPN-24(Fe)**. Meanwhile Fe(II) was oxidized to Fe(III) by the oxygen in air. The color of **PPN-24** also changed from black to dark red due to the presence of Fe(III) ion. The successful incorporation of iron was confirmed by electron dispersive spectroscopy (EDS) (Fig. S10), which proves the high density of active iron-porphyrin centers in **PPN-24(Fe)**.

PPN-24(Fe) possesses all the prerequisites for heterogeneous artificial enzymes: a) a high density of active centers; b) excellent chemical and thermal stability; c) low cost and feasible synthetic procedure. As a probe reaction to evaluate the heme protein biomimetic capacity, the oxidation of 2-2'-azino-bis(3-ethylbenzthiazoline-6-sulfonic acid) (ABTS) to $ABTS^{+\bullet}$ by **PPN-24(Fe)** in the presence of H_2O_2 was examined (Fig. 4a).[13a, 19] The oxidation product can be monitored with the absorbance of the soret band at 418 nm (Fig. 4b) by ultraviolet–visible (UV-Vis) spectroscopy.[20] The reaction was performed with 30 mM ABTS, 10 mM H_2O_2, 5.0 mg/mL **PCN-24(Fe)** in critic buffer at room temperature. The increase of the absorbance at 418 nm well demonstrates the biomimetic activity of **PCN-24(Fe)** in aqueous environment. Meanwhile, we recorded the color change for the whole process, which changed from colorless to dark green in just 15 minutes (Fig. 4c).

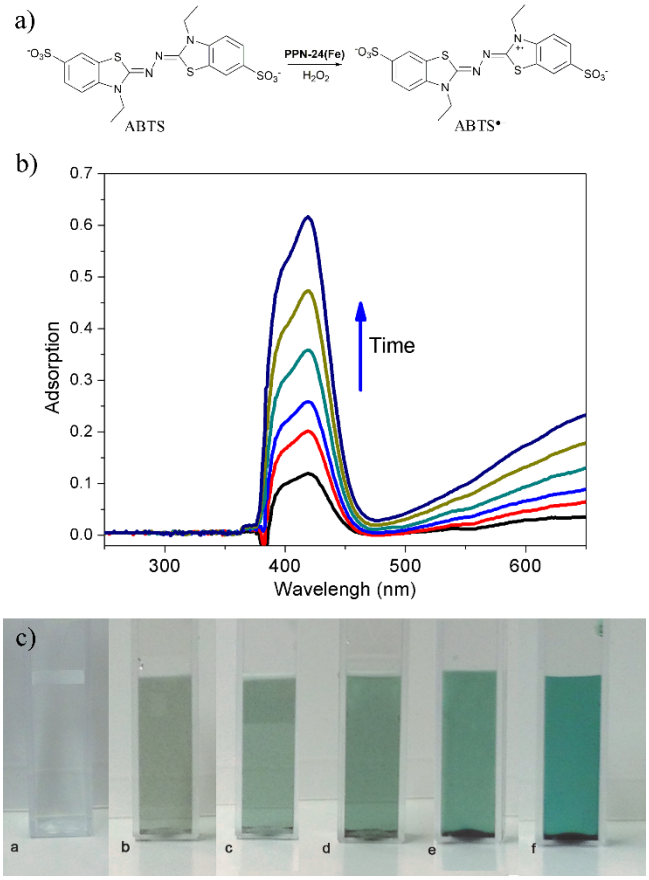

Fig. 4 Oxidation reaction of ABTS catalyzed by **PPN-24(Fe)**. a) The oxidation reaction scheme for ABTS in which ABTS is oxidized to $ABTS^{\bullet+}$ by **PPN-24(Fe)** in the presence of H_2O_2. b) UV-Vis absorbance changes over time for **PPN-24(Fe)** catalyzed ABTS oxidation, and c) The color changes of solution after (a) 1 min, (b) 3 min, (c) 5 min, (d) 7 min, (e) 10 min, (f) 15 min.

In this context, we have successfully demonstrated a facile one-spot synthetic strategy to construct 3D, porous, highly stable **PPN-24(Fe)**, which exhibits great catalytic activity for the oxidation of ABTS. The integration of the high porosity and enhanced thermal and chemical stability in **PPN-24(Fe)** are beneficial for future studies in the synthesis of biomimetic catalytically active PPN materials.

This work was supported as part of the Center for Gas Separations Relevant to Clean Energy Technologies, an Energy Frontier Research Center funded by the U.S. Department of Energy (DOE), Office of Science, Office of Basic Energy Sciences under Award Number DE-SC0001015, part of the Methane Opportunities for Vehicular Energy (MOVE) Program, an ARPA-e project under Award Number DE-AR0000249 and part of the Welch Foundation under Award Number A-1725. The FE-SEM acquisition was supported by the NSF grant DBI-0116835, the VP for Resarch Office, and the TX Eng. Exp. Station. We thank Dr. Muwei Zhang for all the inspiring discussions.

Notes and references:

[a] Department of Chemistry, Texas A&M University, College Station, TX 77842, USA;
[b] Department of Materials Science and Engineering, Texas A&M University, College Station, TX 77843, USA;
Author to whom correspondence should be addressed;
E-Mail: zhou@mail.chem.tamu.edu,

† Electronic Supplementary Information (ESI) available: Detailed synthetic procedure for **PPN-23** and **PPN-24**; pore size distribution of **PPN-24**; experimental details of the FT-IR spectra, TGA measurement, chemical stability and EDS measurements. See DOI: 10.1039/c000000x/

1. D. Mansuy, *C. R. Chim.*, 2007, **10**, 392-413.
2. (a) G. Simonneaux, P. Le Maux, Y. Ferrand and J. Rault-Berthelot, *Coord. Chem. Rev.*, 2006, **250**, 2212-2221; (b) C.-M. Che, V. K.-Y. Lo, C.-Y. Zhou and J.-S. Huang, *Chem. Soc. Rev.*, 2011, **40**, 1950-1975.
3. T. C. Bruice, *Acc. Chem. Res.*, 1991, **24**, 243-249.
4. (a) M. H. Alkordi, Y. Liu, R. W. Larsen, J. F. Eubank and M. Eddaoudi, *J. Am. Chem. Soc.*, 2008, **130**, 12639-12641; (b) J. T. Groves and D. V. Adhyam, *J. Am. Chem. Soc.*, 1984, **106**, 2177-2181; (c) H. Lu and X. P. Zhang, *Chem. Soc. Rev.*, 2011, **40**, 1899-1909.
5. (a) T. Xue, S. Jiang, Y. Qu, Q. Su, R. Cheng, S. Dubin, C.-Y. Chiu, R. Kaner, Y. Huang and X. Duan, *Angew. Chem. Int. Ed.*, 2012, **51**, 3822-3825; (b) Q. Wang, Z. Yang, X. Zhang, X. Xiao, C. K. Chang and B. Xu, *Angew. Chem. Int. Ed.*, 2007, **46**, 4285-4289.
6. (a) O. Leal, D. L. Anderson, R. G. Bowman, F. Basolo and R. L. Burwell, *J. Am. Chem. Soc.*, 1975, **97**, 5125-5129; (b) H. Nagano, M. Matsuda and T. Yajima, *J. Chem. Soc., Perkin Trans. 1*, 2001, 174-182; (c) Z. Li, C.-G. Xia and X.-M. Zhang, *J. Mol. Catal. A: Chem.*, 2002, **185**, 47-56.
7. D. Yuan, D. Zhao, D. Sun and H. C. Zhou, *Angew. Chem. Int. Ed. Engl.*, 2010, **49**, 5357-5361.
8. (a) J.-R. Li, R. J. Kuppler and H.-C. Zhou, *Chem. Soc. Rev.*, 2009, **38**, 1477-1504; (b) E. D. Bloch, W. L. Queen, R. Krishna, J. M. Zadrozny, C. M. Brown and J. R. Long, *Science*, 2012, **335**, 1606-1610.
9. L. E. Kreno, K. Leong, O. K. Farha, M. Allendorf, R. P. Van Duyne and J. T. Hupp, *Chem. Rev.*, 2011, **112**, 1105-1125.
10. (a) H.-C. Zhou, J. R. Long and O. M. Yaghi, *Chem. Rev.*, 2012, **112**, 673-674; (b) D. Feng, Z. Y. Gu, J. R. Li, H. L. Jiang, Z. Wei and H. C. Zhou, *Angew. Chem. Int. Ed. Engl.*, 2012, **51**, 10307-10310.
11. (a) C. Y. Lee, O. K. Farha, B. J. Hong, A. A. Sarjeant, S. T. Nguyen and J. T. Hupp, *J. Am. Chem. Soc.*, 2011, **133**, 15858-15861; (b) A. Fateeva, P. A. Chater, C. P. Ireland, A. A. Tahir, Y. Z. Khimyak, P. V. Wiper, J. R. Darwent and M. J. Rosseinsky, *Angew. Chem.*, 2012, **124**, 7558-7562.
12. D. Yuan, W. Lu, D. Zhao and H. C. Zhou, *Adv. Mater.*, 2011, **23**, 3723-3725.
13. (a) X.-S. Wang, M. Chrzanowski, D. Yuan, B. S. Sweeting and S. Ma, *Chem. Mater.*, 2014, **26**, 1639-1644; (b) A. M. Shultz, O. K. Farha, J. T. Hupp and S. T. Nguyen, *Chem. Sci.*, 2011, **2**, 686-689; (c) L. Chen, Y. Yang and D. Jiang, *J. Am. Chem. Soc.*, 2010, **132**, 9138-9143.
14. A. Modak, M. Nandi, J. Mondal and A. Bhaumik, *Chem. Commun.*, 2012, **48**, 248-250.
15. S. A. Van Arman, *Tetrahedron Lett.*, 2009, **50**, 4693-4695.
16. M. Zhang, Z. Perry, J. Park and H.-C. Zhou, *Polymer*, 2014, **55**, 335-339.
17. N. B. McKeown, S. Hanif, K. Msayib, C. E. Tattershall and P. M. Budd, *Chem. Commun.*, 2002, 2782-2783.
18. S. Ma, D. Sun, X.-S. Wang and H.-C. Zhou, *Angew. Chem. Int. Ed.*, 2007, **46**, 2458-2462.
19. (a) R. W. Larsen, L. Wojtas, J. Perman, R. L. Musselman, M. J. Zaworotko and C. M. Vetromile, *J. Am. Chem. Soc.*, 2011, **133**, 10356-10359; (b) Y. Chen, T. Hoang and S. Ma, *Inorg. Chem.*, 2012, **51**, 12600-12602; (c) M. Zhang, Z.-Y. Gu, M. Bosch, Z. Perry and H.-C. Zhou, *Coord. Chem. Rev.*, 2014.
20. R. W. Noble and Q. H. Gibson, *J. Biol. Chem.*, 1970, **245**, 2409-2413.

Entry for the Table of Contents:

Two stable porphyrin based porous polymer networks (PPNs) were synthesized, and their biomimetic catalytic activities were studied.